Tungsta supported on zirconia and alumina catalysts: temperature-programmed desorption/reaction of methanol and pyridine DRIFTS studies

Gustavo Larsen[1], Srinivasanallur Raghavan, Manuel Márquez and Edgar Lotero

Department of Chemical Engineering, University of Nebraska-Lincoln, Lincoln, NE 68588-0126, USA

Received 31 July 1995; accepted 25 October 1995

The temperature-programmed reaction/desorption of methanol over tungsta supported on zirconia and gamma alumina (WO_3/ZrO_2 and WO_3/γ-Al_2O_3) catalysts was monitored by mass spectrometry. The selectivity toward dimethyl ether (DME) was found to increase and its desorption maxima to shift toward lower temperatures with increasing catalyst acidity. The latter was probed by diffuse reflectance infrared spectroscopy (DRIFTS) of adsorbed pyridine up to 723 K.

Keywords: supported tungsten oxides; methanol temperature-programmed reaction; pyridine DRIFTS studies

1. Introduction

Supported tungsten oxides have long been sought as attractive catalysts for olefin metathesis, acid-catalyzed reactions and as precursors for supported tungsten carbide catalysts [1–8]. Recently, the WO_3/ZrO_2 (WZ) system has been proposed as a good acidic support to produce Pt–WO_3/ZrO_2 reforming catalysts [6]. Hino and Arata [7] indicated that WZ displays superacidic behavior upon calcination at 1073 K, making this material particularly suitable for isomerization of light alkanes. The use of oxoanions other than sulfate (SO_4^{2-}) to increase the acidity of tetragonal zirconia is an active area of research since SO_4^{2-} ions are partially lost during catalyst calcination, regeneration or reduction. From a fundamental viewpoint, it appears interesting to compare the catalytic behavior of WZ and WO_3/γ-Al_2O_3 (WA), given that only the former is known to be a strong solid acid [6,7]. For practical reasons, researchers in the field of oxoanion promotion of zirconia have focussed their attention on isomerization and alkylation of light alkanes. We believe that there is a need for fundamental studies that make use of different chemical and physical probes to help understand the catalytic properties of these materials.

The use of pyridine as a probe molecule to study the acidity of solid materials is a mature technique. During preliminary temperature-programmed desorption (TPD) runs on WZ we noticed that pyridine decomposition above 773 K added an additional complication to this technique. Other nitrogenated bases such as ammonia and isopropyl ammine were also discarded since nitridation of WO_3 would have likely occurred [5] under the temperature-programmed conditions we currently employed. Therefore, we decided to use diffuse reflectance infrared spectroscopy (DRIFTS) of adsorbed pyridine only up to 723 K as the spectroscopic tool for catalyst and catalyst support characterization.

Methanol desorption/reaction was chosen as the test reaction because, unlike higher alcohols, it was a priori expected to produce less olefins (and less coke) as additional dehydration products. In spite of the fact that etherifications do not require very strong acid sites to occur, we found some observations regarding selectivity and desorption behavior worth mentioning. The choice of probe reaction also responds to an interest in exploring other applications for these materials, such as the production of oxygenates from alcohols and olefins or the conversion of methanol to hydrocarbons.

2. Experimental

The preparation of WZ was carried out by a procedure similar to that described in ref. [7]. In brief, a solution of $ZrO_2Cl_2 \cdot xH_2O$ (Aldrich) was used to produce hydrous zirconia (HZ) by precipitation upon addition of 30% NH_3 (Aldrich) to pH 10. The precipitate was filtered and washed with deionized water until no chloride was detected by the $AgNO_3$ test. The solids were then oven-dried at 373 K for 3 h. The HZ material was impregnated to incipient wetness with an aqueous solution of ammonium metatungstate to yield a 12 wt% W material. At this point, the impregnated solid was oven-dried at 373 K again for another 3 h and subsequently calcined for 2 h at 1073 K in a quartz U-tube under an ultra-high purity air flow of 1 ℓ/min g-solid. The selected calcination temperature was achieved in 2 h. For comparison purposes, a W-free zirconia sample (Z) was also

[1] To whom correspondence should be addressed.

produced from HZ following the same calcination protocol. Finally, a γ-Al_2O_3 (A) support from Strem Chemicals was subjected to the same tungsta loading and/or calcination procedures, resulting in samples labeled as A (γ-Al_2O_3 only) and WA (tungsta-loaded material).

Surface area measurements were carried out by the BET method on an adsorption line equipped with greaseless stopcocks, a digital pressure transducer and capable of reaching absolute pressures around 10^{-6} Torr. Prior to BET measurements, samples were outgassed at 723 K for 0.5 h. The infrared spectrum of adsorbed pyridine was obtained on a Nicolet 20SXB FTIR spectrometer at a resolution of 4 cm^{-1}. A diffuse reflectance Fourier transform infrared spectroscopy (DRIFTS) catalytic chamber for in situ experiments and associated alignment mirrors and temperature controller from Spectratech® were used. An all-stainless steel, mass-flow controlled reactor setup that allows for both pulse and flow experiments was connected to the DRIFTS cell. The catalyst powders were reactivated in situ under air at 1073 K for 2 h, and subsequently purged with nitrogen while allowing the DRIFTS cell to cool down to room temperature. Ultra-high purity nitrogen was passed through a bubbler kept at room temperature containing the liquid pyridine (Aldrich) and then allowed in the cell for 0.5 h. The cell was then purged with pure nitrogen for 0.5 h prior to data collection at room temperature, 423, 523, 623 and 723 K.

An MKS quadrupole mass spectrometer (MS) was used for the methanol temperature-programmed reaction (TPReac) experiments. Methanol was allowed in a quartz cell kept at 358 K for 1 h using a similar saturator/reactor setup to that used for pyridine loading of the DRIFTS cell. Prior to the TPReac run, the cell was purged with ultra-high purity helium for another hour. The gas phase was sampled by means of a stainless steel capillary tubing with one end connected to the MS manifold and the other end located at ca. 1 mm above the pelletized (20–45 mesh) catalyst bed. The final temperature (883 K) was achieved by means of a 5.8 K/min ramp. A total of eight masses (m/e = 2, 15, 18, 27, 28, 30, 31 and 45) were followed simultaneously. Masses 31 and 45 correspond to the ($M-1$) peaks of methanol and DME respectively. Masses 28 and 2 were followed to detect the formation of carbon monoxide (CO) and hydrogen (H_2). The mass 27 ($C_2H_3^+$) fragment, which is indicative of higher hydrocarbon production, was not formed during any of the four runs. Masses 28 and 2 also paralleled mass 31 during methanol desorption, but we have verified that they result from alcohol fragmentation in the quadrupole, rather than from catalytic decomposition. In all cases, the shape of the mass 15 TPReac spectra matched in shape that of $m = 45$. There was no methane formation with an identical TPReac fingerprint to that of DME. Rather, the m_{45}/m_{15} ratio of signal simply followed that of a pure DME spectrum. Therefore, we ruled out the formation of methane in detectable amounts during our experiments. Similarly, the $m = 30$ signal followed the same pattern as $m = 31$ in alumina-based catalysts. Thus, formaldehyde did not form in appreciable quantities over these two samples. Methanol, DME, HCHO, CO, H_2, and H_2O were the products detected. This situation differs from similar experiments conducted on HY-zeolite, where a strong $m = 27$ signal ($C_2H_3^+$) was also detected, presumably indicative of olefin formation. The methanol desorption–reaction experiments on HY zeolite will not be included in the interest of brevity. The quadrupole response factors for all masses relative to nitrogen were measured, and a second set of TPReac experiments were conducted to ensure both reproducibility and to calculate the reported selectivities.

3. Results and discussion

Figs. 1a–1d show the methanol TPReac results for all four samples. For simplicity, only masses that showed evidence for the formation of a particular product are plotted. All catalysts displayed evolution of water (resulting from the dehydration pathway) in the range 473–673 K. We have also estimated the irreversibly adsorbed methanol uptake of Z and WZ at 358 K dynamically, by means of pulse injections of the alcohol upstream the TPReac cell. These values, along with the calibrated MS signals and surface areas are reported in table 1. We were unable to estimate accurately the amount of methanol adsorbed by A and WA using the same technique. At 358 K, tailing of the methanol signal that lasted for even a few hours indicated the presence of a broad range of adsorption sites on WA and A. This made precise quantification a difficult task in these two samples. Nevertheless, the relative amounts of methanol that desorbed with and without reaction were estimated using the relative calibration factors.

The Z and WZ catalysts did not show detectable amounts of CO and H_2, whereas A, and to a lesser extent WA, produced significant quantities of these two species that always desorbed toghether at the common temperatures of 700 (A) and 640 (WA) K. The maximum desorption temperature (T_{max}) for DME follows the sequence WZ < WA ≈ Z < A. The WZ catalyst also displays the highest DME selectivity (see table 1). Figs. 1a and 1b also show that a very small amount of HCHO may be formed during the TPReac over WZ and Z ($m/e = 30$, 680 K peak and 520 K shoulder respectively), though its presence was not confirmed by means of other techniques. Overall, this reaction seems to proceed via two major pathways, namely ether formation and decomposition to CO and H_2. It should be pointed out that the CO/H_2 ratio was always less than stoichiometric, suggesting that other carbon-containing species (such as coke or coke precursors) might have been retained on the surface.

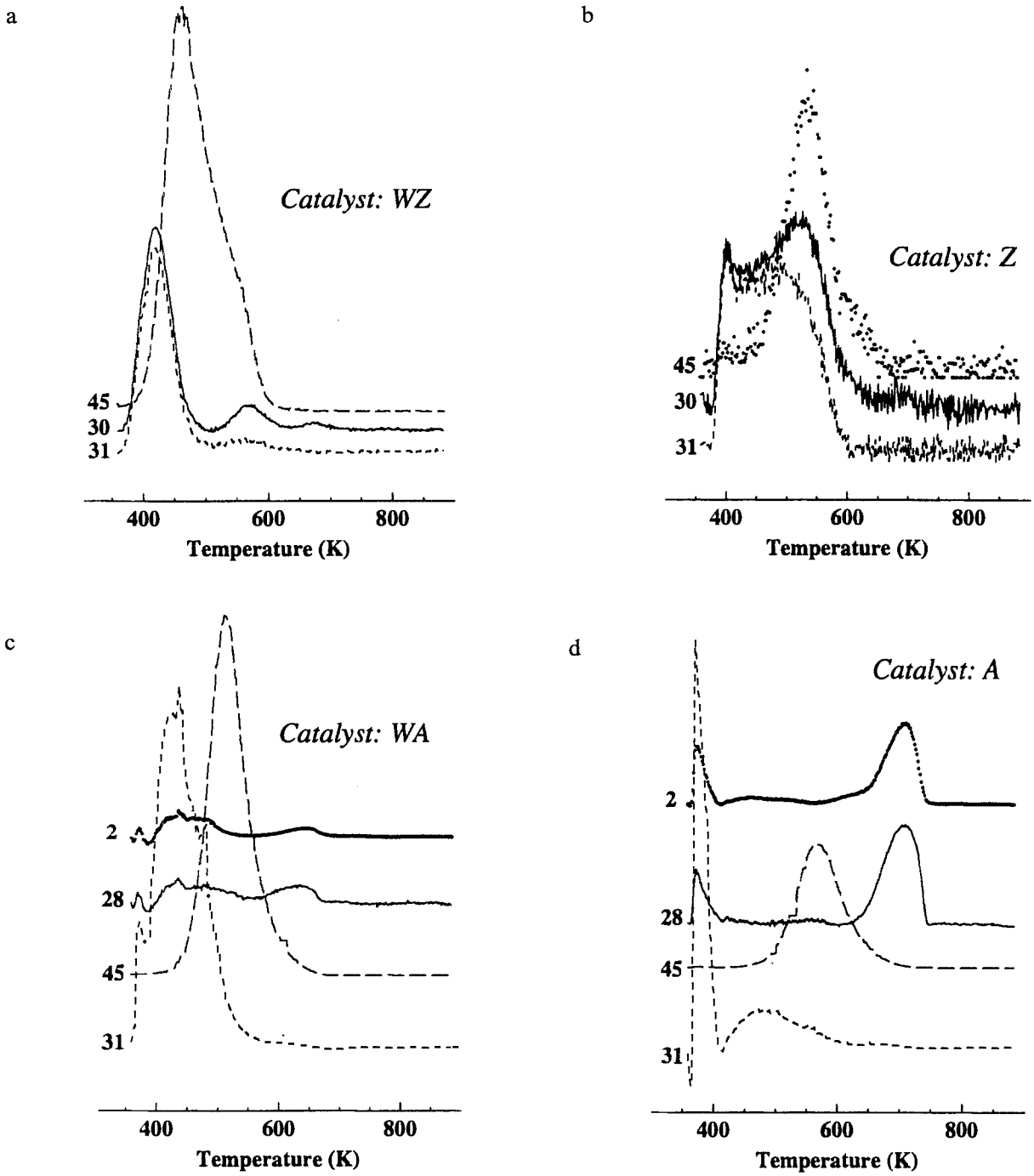

Fig. 1. Temperature-programmed reaction MS data on (a) WZ catalyst showing masses 45 (long dashed), 30 (solid) and 31 (short dashed), (b) Z catalyst showing masses 45 (dotted), 30 (solid) and 31 (short dashed), (c) WA sample showing masses 2 (dotted), 28 (solid), 45 (long dashed) and 31 (short dashed) and (d) sample A with masses 2 (dotted), 28 (solid), 45 (long dashed) and 31 (short dashed).

Table 1
BET surface areas and product yields (μmol/g) during methanol desorption/reaction

Catalyst	$MeOH_{irrev}$	$MeOH_{des}$	DME	CO	H_2	Surface area (m^2/g)
WZ	95	14	35	–	–	45
Z	23	4	6	–	–	9
WA[a]	–	10	9	0.3	0.1	109
A[a]	–	10	8	3	13	118

[a] Since the irreversible methanol uptake of these two catalysts was not measured, product yields are reported per every 10 μmol of MeOH desorbed unreacted.

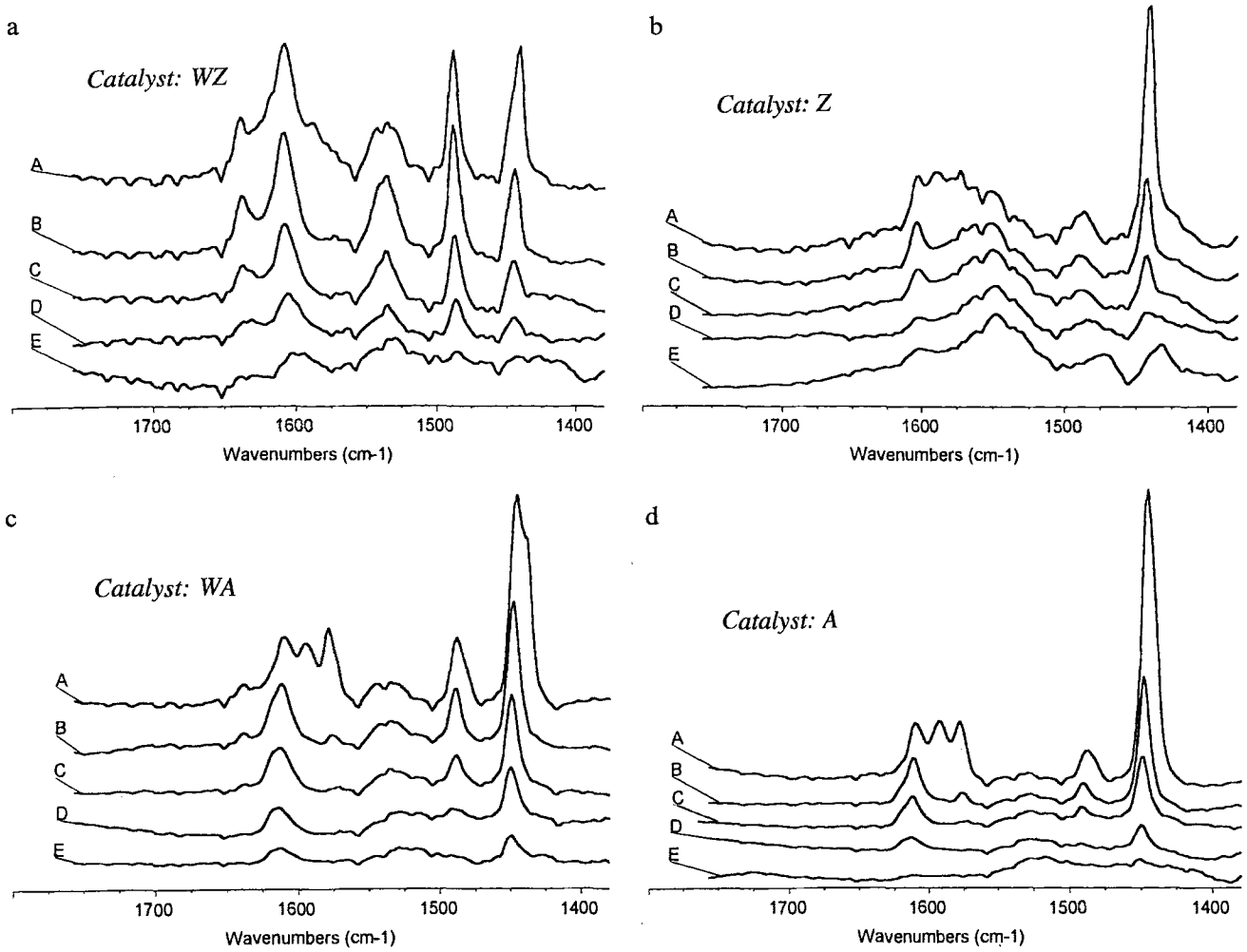

Fig. 2. DRIFTS spectra of adsorbed pyridine on (a) WZ, (b) Z, (c) WA and (d) A catalysts. The A, B, C, D and E labels in all figures correspond to the adsorption temperatures (298, 423, 523, 623 and 723 K respectively).

Figs. 2a–2d show the evolution of the pyridine IR bands with temperature in all four samples. Table 2 shows the assignments for the strong IR absorption bands of pyridine [9]. The spectra at room temperature may not be a good start point for comparison since some weakly bound pyridine may still remain after nitrogen purging. On the other hand, it is immediately apparent that in all cases, the amount of adsorbed pyridine that remained at 723 K was either too small or simply insufficient to guarantee good detection by our DRIFTS setup. An interesting detail is that only WZ presented a shoulder at ca. 1640 cm^{-1} and a broad band around 1535 cm^{-1}, which can be assigned to pyridine bonded to Brønsted acid sites. The strong signal of pyridine adsorbed on WZ at ca. 1488 cm^{-1} cannot be unequivocally assigned to protonated pyridine (see table 2). Another observation is that, judging from the integrated band intensities in table 3, retention of the basic molecule at increasing temperatures seems to follow the trend

Table 2
Pyridine band assignments [a]

Mode	Frequency (cm^{-1})			
	liquid	B [b]	L [c]	H [d]
8a	1579	1631–1640	1602–1632	1580–1600
8b	1572	1600–1613	1575–1585	1577
19a	1478	1478–1490	1478–1490	1480–1490
19b	1439	1530–1550	1445–1460	1440–1445

[a] From ref. [18].
[b] Bonded to a Brønsted acid site.
[c] Bonded to a Lewis acid site.
[d] Hydrogen-bonded pyridine.

Table 3
Relative IR band intensities. Ratios 1 and 2 correspond to $I_{523\,K}/I_{423\,K}$ and $I_{623\,K}/I_{423\,K}$ respectively

Catalyst	Frequency (cm^{-1})					
	1610		1487		1442	
	1	2	1	2	1	2
WZ	0.68	0.30	0.60	0.32	0.53	0.26
Z	0.64	0.24	0.92	0.11	0.48	0.03
WA	0.86	0.42	0.51	0.18	0.53	0.34
A	0.73	0.30	0.33	0.00	0.45	0.15

WZ > WA > Z ≈ A. Note that results in table 3 would underestimate the actual retention of pyridine by WZ, because the 1535 cm^{-1} band (which is unique to this catalyst) has not been included. The pyridine retention sequence also correlates with that of DME T_{max}. In spite of the fact that frequency shifts in the pyridine 8b vibrational mode have been typically associated with the electron-acceptor properties of the solid [10], we have not attempted to correlate such shifts with acidity since this may also be affected by other factors such as adsorbate–adsorbate interactions.

During CO methanation on Pd/Al_2O_3 catalysts, the surface accumulation of methoxy species on the γ-Al_2O_3 support has been demonstrated by both ^{13}C MAS NMR [11], kinetics [12] and infrared spectroscopy [13]. If methanol adsorption on the γ-Al_2O_3 surface proceeds via the formation of methoxy groups, it is conceivable to speculate that its decomposition to CO and H_2 may proceed via one of the inverse steps of the methanation process. The confirmation of such mechanistic analogy is beyond the scope of this work. Nevertheless, the presence of tungsta greatly suppresses the CO/H_2 pathway, which seems to suggest that the sites responsible for this reaction may be affected by interaction with the $-WO_4$ or $-WO_5$ moieties that are found to be present on WA catalysts [14]. By means of X-ray diffraction, we found no evidence for the formation of a separate WO_3 phase on WA and WZ, suggesting that tungsten is in a well-dispersed state [14,15].

As expected, WZ appears to be the most acidic material. Given the fact that Brønsted acidity seems to be present only in the case of WZ, the high reactivity toward DME formation of this catalyst may be attributed to this factor. However, we have also carried out experiments using an HY-zeolite catalyst (not shown) which also possesses Brønsted acidity and an *n*-butane isomerization activity comparable to that of WZ, and found that the DME T_{max} occurred at 510 K (30 K above that of WZ) with a selectivity that resembles that of WA. In addition, pronounced coking was apparent in the case of HY which turned dark grey after the TPReac experiment and also produced a large $m/e = 27$ signal which can only correspond to a $C_2H_3^+$ fragment. In fact, acidic zeolites are known to yield ethylene and higher olefins from methanol [16]. On the other hand, the WZ catalyst experienced no color change with respect to its pale green calcined form after the TPReac experiments. A natural consequence of these observations is that WZ is less likely to be a better methanol-to-olefins (MTO) or methanol-to-gasoline (MTG) catalyst than acidic zeolites, but its potential for other acid-catalyzed reactions such as methyl- and ethyl-tert-butyl-ethers (MTBE or ETBE) syntheses remains to be tested.

In order to accept the idea that the DME T_{max} correlates with catalyst acidity, the surface has to display very low chemisorption affinity for the product molecule. In recent studies, we noticed that ethers such as ETBE are not adsorbed molecularly onto the acid sites of zeolites at 338 K [17]. Therefore, we do not expect DME to chemisorb on the surface of the catalysts and to present a T_{max} indicative of a slow desorption process. One of the issues that we wish to address in the future is to see how WZ will rank among a number of solid acid catalysts by means of several chemical and physical probes. The superacidity of sulfated zirconia has recently been questioned in light of spectroscopic evidence [18], and it is conceivable that WZ is also in the strong acid rather than in the superacidic range.

4. Conclusion

The presence of tungsten on zirconia and alumina surfaces increases the pyridine retention at high temperatures and improves the reactivity and selectivity toward DME formation during temperature-programmed reaction of methanol. Zirconia-supported tungsta is the most reactive sample toward DME formation as evidenced from the lower reaction–desorption temperature profile.

Acknowledgement

This work was funded in part by the Petroleum Research Fund of the American Chemical Society under grant # 28336-G5 and by the Nebraska-EPSCoR (NSF, grant # OCR-9255225) supplement to GL's NSF-RIA award (CTS-9406718). We also thank the University of Nebraska Research Council and Layman Fund for generous support. One of us (EL) would like to express his appreciation to COLCIENCIAS (Colombian Research Council) for his visiting scholarship award.

References

[1] A.G. Basrur, S.R. Patwardhan and S.N. Vyas, J. Catal. 127 (1991) 86.
[2] R.C. Luckner, G.E. McConchie and G.B. Wills, J. Catal. 28 (1973) 63.
[3] S.J. Choung and S.W. Weller, Ind. Eng. Chem. Prod. Res. Dev. 22 (1983) 662.
[4] B.M. Reddy and K.S. Prasad Rao, J. Catal. 113 (1988) 556.
[5] M.J. Ledoux, C.P. Huu, J. Guille and H. Dunlop, J. Catal. 134 (1992) 383.
[6] S.L. Soled, AIChE 1994 Annual Meeting, paper 85f, San Francisco, November 1994.
[7] M. Hino and K. Arata, J. Chem. Soc. Chem. Commun. (1987) 1259.
[8] P. Patel, A. Shivanekar and U. Chudasama, Indian J. Chem. 31A (1992) 803.
[9] G. Connell and J.A. Dumesic, J. Catal. 101 (1986) 103.
[10] C. Morterra and G. Cerrato, Langmuir 6 (1990) 1812.
[11] O.H. Han, G. Larsen, K.W. Zilm and G.L. Haller, in: *New Aspects of Spillover Effect in Catalysis*, ed. T. Inui (Elsevier, Amsterdam, 1993) p. 223.

[12] E.C. Hsiao and J.L. Falconer, J. Catal. 132 (1991) 145.
[13] J. L. Robbins and E. Marucchi-Soos, J. Phys. Chem. 93 (1989) 2885.
[14] F. Hilbrig, H.E. Göbel, H. Knözinger, H. Schmeltz and B. Lengeler, J. Phys. Chem. 95 (1991) 6973.
[15] J.A. Horsley, I.E. Wachs, J.M. Brown, G.H. Via and F.D. Hardcastle, J. Phys. Chem. 91 (1987) 4014.
[16] N.Y. Chen and W.J. Reagan, J. Catal. 59 (1979) 123.
[17] G. Larsen, E. Lotero and H.S. Silva, J. Catal., submitted.
[18] V. Adeeva, J.W. de Haan, J. Jänchen, G.D. Lei, V. Schünemann, L.J.M. van de Ven, W.M.H. Sachtler and R.A. van Santen, J. Catal. 151 (1995) 364.